INVESTIGATION OF SHALLOW BULK ACOUSTIC WAVES

FINAL REPORT

K. H. YEN, R. S. KAGIWADA, K. F. LAU,
AND R. B. STOKES

12 NOVEMBER 1981

U.S. Army Research Office

Contract No. DAAG26-78-C-0043

TRW Defense and Space Systems Group
One Space Park, Redondo Beach, California 90278

TRW
DEFENSE AND SPACE SYSTEMS GROUP

THE FINDINGS IN THIS REPORT ARE NOT TO BE CONSTRUED AS AN OFFICIAL DEPARTMENT OF THE ARMY POSITION, UNLESS SO DESIGNATED BY OTHER AUTHORIZED DOCUMENTS.

12

INVESTIGATION OF SHALLOW BULK ACOUSTIC WAVES

FINAL REPORT

K. H. YEN, R. S. KAGIWADA, K. F. LAU,
AND R. B. STOKES

12 NOVEMBER 1981

U.S. Army Research Office

Contract No. DAAG26-78-C-0043

TRW Defense and Space Systems Group
One Space Park, Redondo Beach, California 90278

TRW
DEFENSE AND SPACE SYSTEMS GROUP

Unclassified

SECURITY CLASSIFICATION OF THIS PAGE (When Data Entered)

REPORT DOCUMENTATION PAGE		READ INSTRUCTIONS BEFORE COMPLETING FORM
1. REPORT NUMBER	2. GOVT ACCESSION NO. AD-A109 028	3. RECIPIENT'S CATALOG NUMBER
4. TITLE (and Subtitle) Investigation of Shallow Bulk Acoustic Waves		5. TYPE OF REPORT & PERIOD COVERED Final Report 1 Oct. 1978 - 19 Sept. 1981
		6. PERFORMING ORG. REPORT NUMBER
7. AUTHOR(s) K. H. Yen, R. S. Kagiwada, K. F. Lau, and R. B. Stokes		8. CONTRACT OR GRANT NUMBER(s) DAAG26-78-C-0043
9. PERFORMING ORGANIZATION NAME AND ADDRESS TRW Defense and Space Systems Group One Space Park, Redondo Beach, CA 90278		10. PROGRAM ELEMENT, PROJECT, TASK AREA & WORK UNIT NUMBERS
11. CONTROLLING OFFICE NAME AND ADDRESS U. S. Army Research Office Post Office Box 12211 Research Triangle Park, NC 27709		12. REPORT DATE November 12, 1981
		13. NUMBER OF PAGES
14. MONITORING AGENCY NAME & ADDRESS(if different from Controlling Office)		15. SECURITY CLASS. (of this report) Unclassified
		15a. DECLASSIFICATION/DOWNGRADING SCHEDULE NA

16. DISTRIBUTION STATEMENT (of this Report)

Approved for public release; distribution unlimited.

17. DISTRIBUTION STATEMENT (of the abstract entered in Block 20, if different from Report)

NA

18. SUPPLEMENTARY NOTES

The findings in this report are not to be construed as an official Department of the Army position, unless so designated by other authorized documents.

19. KEY WORDS (Continue on reverse side if necessary and identify by block number)

Shallow bulk acoustic wave, Bleustein-Gulyayev wave, rotated Y-cut quartz, berlinite, $LiTaO_3$, $LiNbO_3$, wave velocity, piezoelectric coupling constant, temperature stability, filters, oscillators.

20. ABSTRACT (Continue on reverse side if necessary and identify by block number)

This final report summarizes the most important results of the Investigation of Shallow Bulk Acoustic Waves (SBAW) program, under ARO Contract DAAG26-78-C-0043. This program was conceived on the principle that SBAW technology could lead to devices that are superior to those presently available for frequency filtering and control. The primary objective was to establish whether this technology could provide devices that were as stable as the low frequency bulk wave resonators and yet operate at frequencies higher than the surface acoustic wave devices. (Cont'd)

DD FORM 1 JAN 73 1473 EDITION OF 1 NOV 65 IS OBSOLETE

Unclassified

SECURITY CLASSIFICATION OF THIS PAGE (When Data Entered)

This program has clearly met all of the objectives. We have theoretically and experimentally investigated shallow bulk acoustic waves in terms of material aspects, equivalent circuit and device development. Our investigations have shown that SBAW devices can be built with excellent temperature stability, low spurious modes and at frequencies higher than those of SAW devices and bulk wave resonators.

FOREWORD

This program was conceived on the principle that Shallow Bulk Acoustic Wave (SBAW) technology could lead to devices that are superior than those presently available for frequency control. The aim was to establish whether this technology could provide devices that were as stable as the low frequency bulk wave resonators and yet operate at frequencies higher than the surface acoustic wave devices.

This Army Research Office program entitled "Investigation of Shallow Bulk Acoustic Waves" has already met all of these objectives. Our investigations have shown that SBAW oscillators can be built with excellent temperature stability and at frequencies higher than those of SAW oscillators. This program has also demonstrated that a new family of filters can be built with superior characteristics. This report will amplify on these comments.

CONTENTS

LIST OF FIGURES

LIST OF FIGURES (Cont'd)

LIST OF TABLES

1.0 INTRODUCTION

This final report summarizes the most important results of the investigation of Shallow Bulk Acoustic Waves (SBAW) program under ARO contract DAAG26-78-C-0043. Shallow bulk acoustic waves are shear horizontal waves which propagate closely to the surface of the substrate. Using these waves, a new family of planar bulk wave devices which possess many inherent advantages over conventional bulk and surface acoustic wave devices can be realized. These devices can be employed as bandpass filters and oscillators, and thus can be incorporated into a variety of signal processing systems.[1,2,3]

For years, the interdigital transducers have been successfully used in the rapidly developing field of Surface Acoustic Waves (SAWs). This led to the development of various planar SAW devices for military electronic systems. One of the main difficulties encountered in such SAW devices arises from the fact that interdigital transducers can efficiently generate and detect bulk waves as well as surface acoustic waves. For SAW devices, the generation of bulk waves is undesirable, especially when high out-of-band rejection is required. Thus, bulk wave excitation in SAW devices has been theoretically and experimentally investigated in order to develop techniques to suppress it.[4,5,6]

During the course of our SAW device investigation, we realized that bulk waves can also play a useful role in device applications. By choosing the correct piezoelectric material and crystallographic orientation, we have observed that these waves can be efficiently generated and detected using interdigital transducers similar to those used for SAW devices.[1,2] These waves are confined to a region close to the

surface and they are beamed directly from one transducer to the other. On rotated Y-cut quartz, with the interdigital transducer fabricated 90° from the X-axis, these shallow bulk acoustic waves can be generated and detected at frequencies up to three times higher than those of SAW devices.

This final report is divided into five sections. Section 1 is the introduction. Section 2 provides a brief description of program objectives. Section 3 describes properties of shallow bulk acoustic waves, including material aspects, excitation, propagation, and detection. In the material area, the most promising substrates for SBAW devices are quartz, berlinite, lithium tantalate ($LiTaO_3$), and lithium niobate ($LiNbO_3$). Quartz, $LiTaO_3$, and $LiNbO_3$ are well established materials for surface acoustic wave devices. Because quartz is of great importance for temperature stable SBAW devices, it was extensively investigated and is discussed in Section 3.2. Since berlinite is a relatively new acoustic wave material, its SBAW properties and qualities have been thoroughly studied for the first time, and the important results are given in Section 3.3. Also in Section 3, an "in-line" equivalent circuit model is presented for SBAW transducers.

Section 4 discusses SBAW device development, including narrowband and wideband filters and high frequency oscillators. SBAW filters with excellent performance have been fabricated on quartz and $LiTaO_3$.[7] Stable 2 GHz and 3.4 GHz SBAW oscillators have been constructed,[8] and are shown in Section 4.3.

This is followed by the conclusions (Section 5), and a list of publications under this program.

2.0 OBJECTIVE

The objective of this program is to investigate the properties of Shallow Bulk Acoustic Waves, emphasizing those properties which will lead to fabrication of SBAW devices that have future signal processing applications. More specifically, the objectives include:

- o Further understanding and characterization of the shallow bulk acoustic wave in terms of its generation and detection and its propagation properties in piezoelectric solids.
- o Establishing an equivalent circuit model for the SBAW so that optimum SBAW devices can be routinely designed for each specific application.
- o A search for materials and propagation orientations that possess good temperature stability and/or high piezoelectric coupling to be used as substrates for SBAW devices.
- o Fabrication of SBAW devices to verify their performances as compared to those of similar SAW devices. These include bandpass filters, resonators, oscillators and grating devices.

All of these objectives have been achieved in this program. We have extensively analyzed the nature of shallow bulk acoustic waves, Bleustein-Gulayev (B-G) waves and leaky B-G waves in piezoelectric solids.[9] A complete understanding of their interaction and propagation has led us to establish a simple equivalent circuit model for SBAW transducers. This equivalent circuit has been routinely used to design SBAW devices. In the material area, we have investigated many acoustic wave substrate crystals. The most promising substrates are quartz, berlinite, $LiTaO_3$, and $LiNbO_3$. Among these materials, quartz is of paramount importance for temperature-stable device applications. Our device development has shown that SBAW filters and oscillators are in many respects better than SAW devices. They have higher frequency of operation, better temperature

stability, and better spurious bulk wave rejection. For example, a temperature stable SBAW oscillator has been constructed and directly operated at 3.4 GHz. This device represents the highest frequency source ever built using SBAW or SAW technology. The result also indicates that the frequency of operation of SBAW oscillators can be extended to 5 GHz. In addition, we were the first to incorporate a metallic grating in SBAW devices for reduction of insertion loss by energy trapping.[7] Thus, SBAW devices with energy trapping gratings can be used to produce bandpass filters with low insertion loss, high ultimate out-of-band rejection, and better temperature stability.

3.0 NATURE OF SHALLOW BULK ACOUSTIC WAVES

This section describes the investigation of SBAW properties, excitation, propagation and detection. The most promising substrates for SBAW devices are still quartz, berlinite, $LiTaO_3$ and $LiNbO_3$. A thorough investigation was made (see Section 3.2) on quartz, since it is the most temperature stable material. It is also well-established and is widely used in both bulk wave resonators and surface acoustic wave devices. Since berlinite is a relatively new material, a detailed study of berlinite is given in Section 3.3. In addition, an equivalent circuit model has been obtained for SBAW transducers. This equivalent circuit is routinely used to design SBAW devices.

3.1 SBAW Materials

Shallow bulk acoustic wave devices utilize shear horizontal waves which propagate just below the surface of the substrate. Thus, the important criteria used in selecting SBAW materials are:

1) Large piezoelectric coupling to shear horizontal wave
2) Zero or small temperature coefficient of delay
3) Zero or small piezoelectric coupling to SAW and other bulk waves
4) Zero or small beam steering both on the surface and into the bulk.

Using these criteria, we have evaluated several substrate materials. To date, the best SBAW substrates are those commonly employed by SAW devices; i.e., quartz, berlinite, lithium tantalate ($LiTaO_3$), and lithium niobate ($LiNbO_3$).

The suitable cuts of $LiTaO_3$ and $LiNbO_3$ are listed in Table 1. These employ shear horizontal waves propagating along the X-axis in the infinite medium. At these cuts, the transducer can only strongly excite and detect the shear horizontal wave. These waves do not suffer any beam steering on the surface ($\phi_{12} = 0$) and into the medium ($\phi_{13} = 0$). Previous work on shear horizontal (S-H) type surface waves has also indicated the existence of isolated SAWs on the free surface near these cuts.[10,11] Thus, the dominant mode of wave propagation in these crystals is the shear horizontal bulk wave traveling near the surface. As a result, they are considered as SBAW.

Table 1. SHEAR HORIZONTAL WAVES ON $LiTaO_3$ AND $LiNbO_3$

	$LiTaO_3$		$LiNbO_3$	
Euler Angles	$\lambda=0,\mu=35,\theta=0$	$\lambda=0,\mu=54.9,\theta=0$	$\lambda=0,\mu=37.93,$ $\theta=0$	$\lambda=0,\mu=52.27,$ $\theta=0$
Velocity M/Sec	4211.6	3367.09	4802.88	5058.97
k^2 (%)	4.7	1.9	16.7	-
Power Flow Angles ϕ_{12}	0	0	0	0
ϕ_{13}	0	0	0	0
First Order Temperature Coefficient of Delay (PPM/°C)	45	63	59	79

The wideband SBAW delay lines were fabricated on $LiTaO_3$, which has a much higher piezoelectric coupling constant than that of quartz. Frequency responses of these wideband devices are given in Section 4.

For singly rotated Y-cut quartz and berlinite, the above criteria are satisfied with wave propagation normal to the X-axis. Here, the SAW and other bulk waves coupling coefficients are identically zero, so that they are free of spurious responses. In addition, the shear horizontal wave suffers no beam steering on the surface, and for two small regions near AT- and BT-crystal, both the temperature coefficients of delay and beam steering into the substrate are very small. Thus, these regions are especially useful for narrowband filters and oscillator applications.

SBAW or doubly rotated cut quartz has been reported by Ballato and Lukaszek[12] and Ballato, et.al.[13] In addition to excellent temperature behavior, SBAW on doubly rotated cut quartz also potentially possess nonlinear mechanical and thermal stress-compensating effects similar to those of the SC-cut bulk crystal. so they are ideally suited for applications where low aging is required.

Because of important applications of stable narrowband filters and oscillators, a detailed analysis of SBAW on quartz and berlinite is given in the next two sections.

3.2 SBAW in Quartz

Quartz is a natural choice for analysis because it is so widely used in industry for frequency control. It is employed for oscillators and filters for bulk wave as well as surface wave devices. In this section,

we solve for important parameters on quartz such as velocity, insertion loss using an equivalent circuit, and coupling coefficient, and temperature coefficient of delay.

3.2.1 SBAW Velocity

By solving the Christoffel Equations and taking into consideration boundary conditions, one can show that for rotated Y-cut quartz the longitudinal and vertical shear acoustic modes are decoupled from the electric potential. As a result, the modes of interest inside the quartz medium are the horizontal shear quasi-acoustic mode and the quasi-electrostatic mode. They are coupled through the piezoelectric constant and neither of them is purely acoustic or electrostatic.

Figure 1 shows the theoretical calculated SBAW velocity with power flow along the surface.[9] The velocity of the bulk wave with the k vector pointing along the surface is also plotted for comparison. The experimental points agree well with the calculated SBAW velocity.

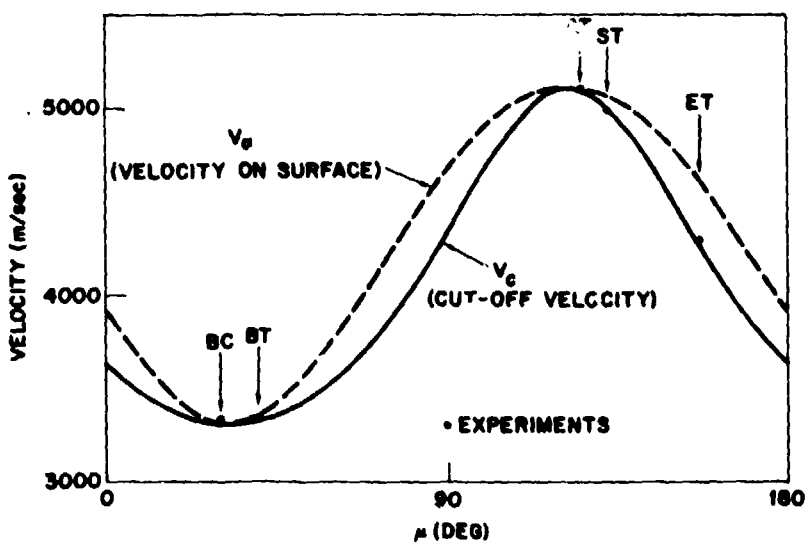

Figure 1. CUTOFF VELOCITY AND VELOCITY ON SURFACE OF HORIZONTALLY POLARIZED SHEAR WAVE ON ROTATED Y-CUT QUARTZ

In addition to SBAWs, Bleustein-Gulayev (B-G) waves and leaky B-G waves also exist in rotated Y-cut quartz.[14] B-G waves consist of a linear combination of the decaying (in a direction normal to the crystal surface) quasi-electrostatic and quasi-acoustic modes. These B-G waves exist on rotated Y-cut quartz for the crystal orientations of 0° to 14.5° and 138° to 180° (Fig. 2). However, in the orientation region 14.5° to 138°, leaky B-G waves exist with the acoustic velocity lower than the bulk wave cut-off velocity. The waves consist of a linear combination of the quasi-acoustic and quasi-electrostatic modes; the electrostatic mode is nearly evanescent, its decay length being on the order of the acoustic wavelength, and the quasi-acoustic mode is slowly leaking into the substrate. The existence of the leaky wave solution is important for a rigorous SBAW analysis.[14]

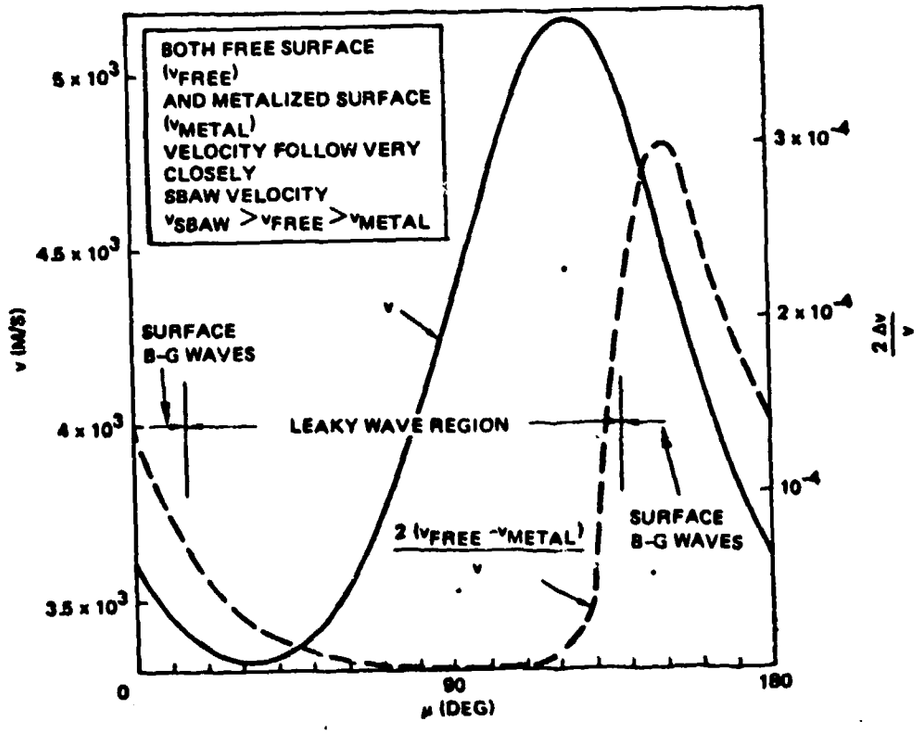

Figure 2. VELOCITY AND $2\Delta v/v$ FOR THE (LEAKY) SURFACE B-G WAVES IN ROTATED Y-CUT QUARTZ

3.2.2 Equivalent Circuit Model of SBAW Transducers

The configuration of a SBAW device on rotated Y-cut quartz is shown schematically in Figure 3. Interdigital transducers are deposited on the substrate surface with fingers parallel to the X-axis of the quartz crystal. SBAWs propagate in the crystalline YZ plane and are detected by a receiving transducer situated at a center-to-center distance r away.

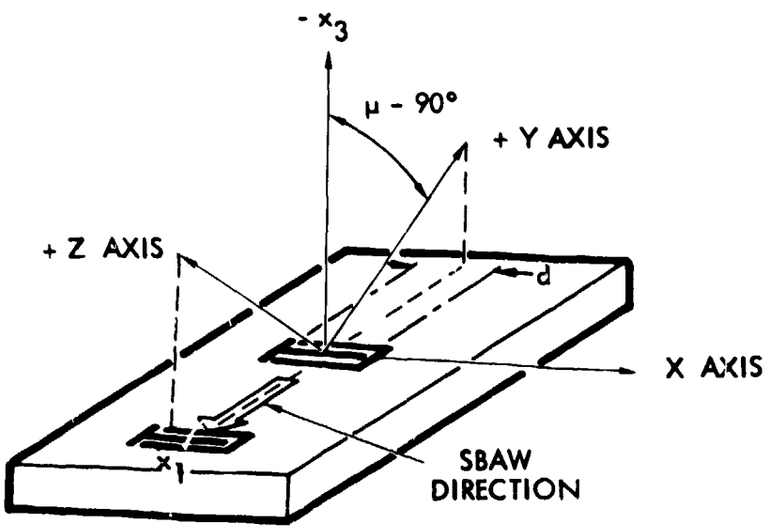

Figure 3. GEOMETRY OF A SBAW DEVICE ON ROTATED Y-CUT QUARTZ; μ = 132.75 FOR ST-CUT QUARTZ

The analysis of acoustic waves excited by the interdigital transducer consists of (1) determining the radiation characteristics of a single line source (element factor); and (2) summing the contributions from these individual sources (array factor). In this approach, the interdigital transducer is represented by a series of parallel line sources with alternate polarity.[9]

It has been shown that, at center frequency, the radiation resistance of the transducer is given by[9]

$$R_a(\omega_c) = \frac{2}{\pi} \frac{K_p^2}{\sqrt{N}} \frac{1}{\omega_c C_s} \tag{1}$$

where C_s is the capacitance per finger pair, and K_p^2 and ω_c are the piezoelectric coupling constant of SBAW and radian resonance frequency of the interdigital transducer. The K_p^2 is obtained from the SBAW Poynting vector and it is not the same as $2\Delta v/v$, where Δv is the velocity difference of the SBAW with and without considering the piezoelectric effect.[7,9] Figure 4 shows the $\Delta v/v$ and the K_p^2 for the SBAW in rotated Y-cut quartz. For certain cuts, these two quantities are comparable, while at other cuts they can differ by an order of magnitude.

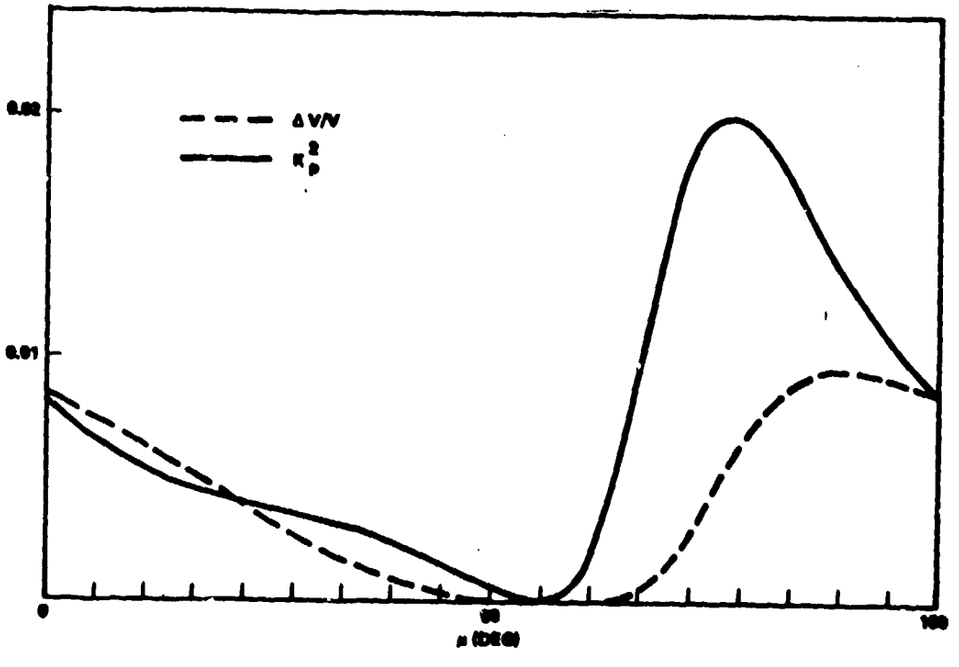

Figure 4. $\Delta v/v$ AND K_p^2 OF SBAW IN ROTATED Y-CUT QUARTZ

The expression derived for the radiation resistance can be used to construct an equivalent circuit. In this model, the SBAW transducer is represented by radiation resistance in series with the capacitance C_T as shown in Figure 5.

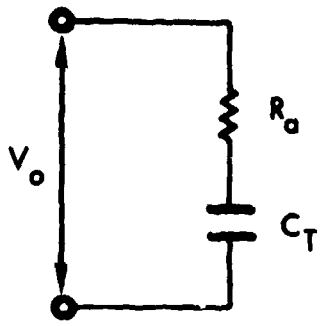

$$R_a \cong \frac{2}{\pi} \frac{1}{\sqrt{N}} K_p^2 \frac{1}{\omega_c C_s}$$

$$C_T = N C_s$$

$$I.L = C.L._1 + C.L._2 + S.L.$$

Figure 5. EQUIVALENT CIRCUIT MODEL FOR A SBAW TRANSDUCER ON QUARTZ

It is interesting to point out that the R_a in this SBAW model is quite similar to that used in the "in-line" model for SAW devices. The major difference is the fact that the effective coupling of the SBAW is inversely proportional to $\sqrt{N}$ while it is independent of N for the SAW case.

3.2.3 Insertion Loss

The insertion loss of the SBAW device is the sum of three contributions: conversion loss of the input transducer, conversion loss of the

output transducer, and acoustic spreading loss. Employing the equivalent circuit of Figure 5, the untuned conversion loss of a transducer is calculated by

$$C.L. = 10 \log \frac{2R_a R_L}{(R_a + R_L)^2 + (\frac{1}{\omega_c C_T})^2} \tag{2}$$

Here the 3 dB bidirectional loss is included. For SBAW devices, an additional loss is included. This loss is related to the acoustic loss. Because the SBAW is a shear horizontal bulk wave, it radiates power into the substrate when it propagates from the input transducer to the output transducer. Thus, the acoustic loss is defined as the ratio of the total received power divided by the total radiated power.

To a good approximation, the power received by the output transducer may be calculated by using the reciprocity arguments. For identical output and input transducers, the acoustic loss, AL, under matched load conditions is shown as[7,9]

$$A.L. = 10 \log \frac{\lambda_c N}{4.5r} \tag{3}$$

where λ_c is the SBAW wavelength. We note that Eq. (3) implies a minimum insertion loss attainable when two identical transducers are placed in close proximity with the center-to-center distance $r = N\lambda_c$. Under matched load conditions,

$$AL_{min} = 10 \log \frac{1}{4.5} \approx 6.5 \text{ dB} \tag{4}$$

This includes the 6 dB bidirectional loss in the transducer. In practice, it is not possible to reach AL_{min}, since, in the limit where (4) was derived, the far-field approximation is not valid.

Not all the acoustic energy radiated toward the output transducer is received. This so-called acoustic power spreading loss is equal to the acoustic loss given by Eq. (3) minus 6 dB, as this has been included in the transducer conversion loss. The expression for the spreading loss is thus given by

$$S.L. = 10 \log \frac{\lambda_c N}{4.5r} - 6. \tag{5}$$

The total insertion loss is then given by

$$IL = C.L._1 + C.L._2 + S.L. \tag{6}$$

Using this equivalent circuit model, the insertion loss of delay lines fabricated on various rotated Y-cut quartz has been calculated and agrees well with experiment. Table 2 summarizes the result. This equivalent circuit model is now routinely used to design SBAW devices.

Table 2. CALCULATED AND MEASURED INSERTION LOSS (λ=0°, θ=90°)

		Theoretical Calculation			
Substrates	μ (Deg)	Conversion Loss Per Transducer	Spreading Loss	Total Insertion Loss	Measured Insertion Loss
ET	156.3	11.2 dB	1.3 dB	23.7 dB	21.8 dB
ST	132.75	9.9	1.3	21.1	22.0
AT	125.25	11.0	1.3	23.3	25.0
BT	41.0	17.3	1.3	35.9	37.2
BC	30.0	16.5	1.3	34.3	32.0

3.2.4. Temperature Coefficient of Delay

The temperature coefficient of delay can be calculated once the correct value of V_{SBAW} is found. The procedure for the temperature coefficient calculation consists of first evaluating the piezoelectric, elastic, and dielectric constants, and density of the quartz substrate at various temperatures. The temperature coefficients of all these quantities have been well documented.[15] After the correct material constants were determined, V_{SBAW} at the particular temperature was calculated. The oscillation condition of the SBAW delay line oscillator is used to compute the frequency shift. A polynomial fit is then carried out to fit the f(T)'s with 1st, 2nd, and 3rd order temperature coefficients of frequency ($\Delta f/f$). The temperature coefficient of delay ($\Delta\tau/\tau$) is merely the negative of that quantity.

For the SBAW in rotated Y-cut quartz, the first order temperature of delay at 25°C is plotted in Figure 6. The agreement between theory and experiment is excellent. For device applications, the regions where zero first order temperature coefficient exists is of great importance. A detailed calculation has been made for cuts near AT and BT cuts which have

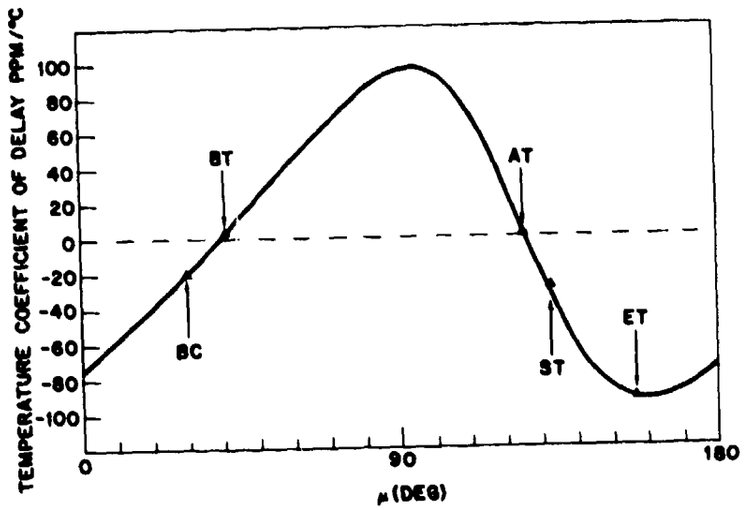

Figure 6. FIRST-ORDER TEMPERATURE COEFFICIENT OF DELAY OF SBAW IN ROTATED Y-CUT QUARTZ

zero first order temperature coefficients of delay. The frequency shift as a function of temperature for the AT cut region is shown in Figure 7, while Figure 8 shows the temperature shift for the BT-cut region. The results again agree well with experiments.

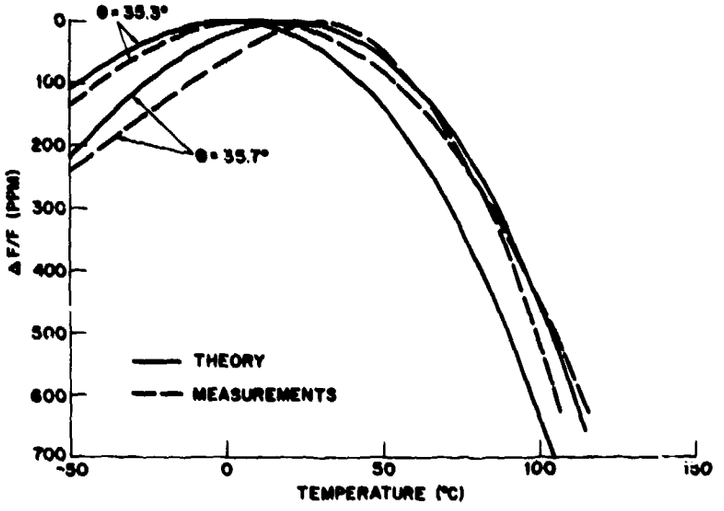

Figure 7. TEMPERATURE SHIFT IN FREQUENCY FOR CUTS NEAR AT-CUT

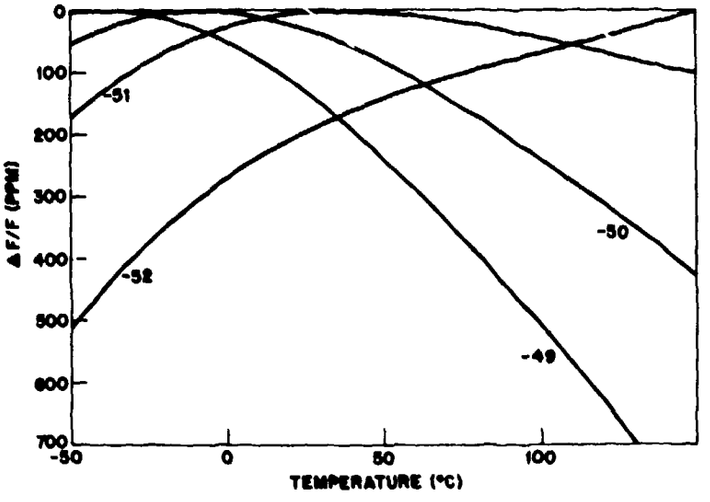

Figure 8. CALCULATED TEMPERATURE SHIFT IN FREQUENCY FOR CUTS NEAR BT-CUT

3.3 SBAW in Berlinite

Berlinite has the same symmetry as quartz and can be analyzed using similar techniques. The calculated V_{SBAW} and K_p^2 for berlinite are shown in Figures 9 and 10, respectively. The computer calculations used the measured material constants by Chang and Barsh.[16] The wave velocity is smaller than that of quartz, but K_p^2 is in general 2.8 times higher. Figure 11 shows the theoretical calculated first order temperature coefficient of delay of rotated Y-cut berlinite. In general, the shape is quite similar to quartz. These results mean that berlinite is suitable for stable wideband devices.

Investigations of detailed acoustic wave properties in berlinite have, however, been hampered by the lack of high quality single crystals with adequate sizes. Recent advances in crystal growth have made available samples with adequate quality and dimensions for further eval ation. Several berlinite substrates were provided to TRW by Allied Chemicals for evaluation. The results represent the first theoretical and experimental analysis of quality of berlinite for SBAW devices.

The calculated result shown in Figures 9-11 indicated that temperature stable cuts occur in two regions of the rotation angle θ, +40.5° and -64°. We have therefore chosen these two orientations for investigations. In addition, substrates with θ equal to 39.5°, 40°, and 41° and 41.5° were also selected to allow determination of orientation dependences of various wave quantities.

3.3.1 +40.5° Rotated Y-Cut Berlinite

Figure 12 shows the frequency response of a SBAW delay line fabricated on 40.5° rotated Y-cut berlinite. The unmatched insertion loss of the device was 22 dB. The response shape was a $(\sin x/x)^2$ function and few spurious signals were observed.

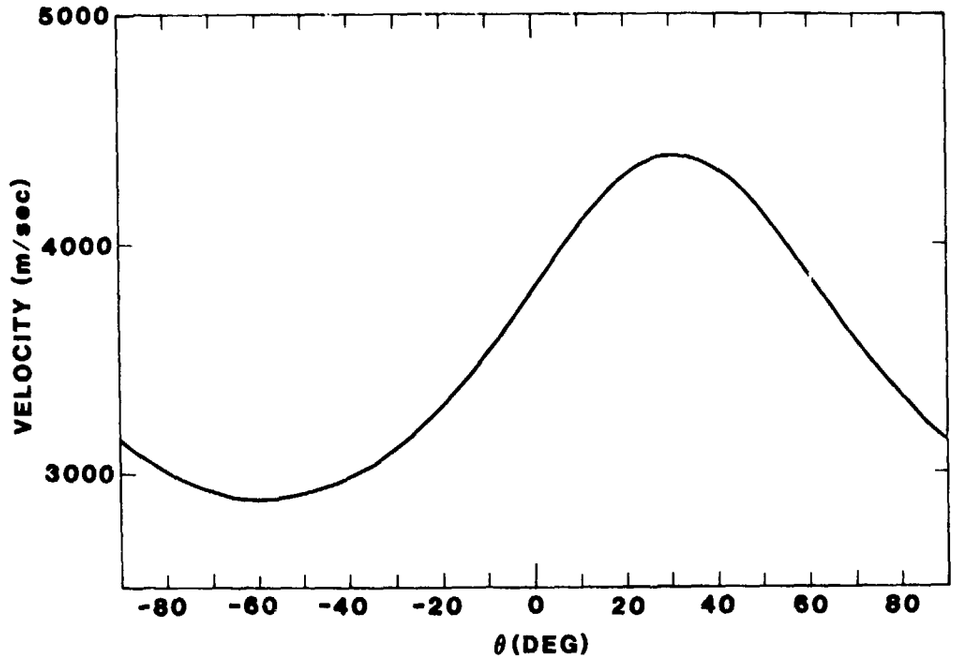

Figure 9. CUTOFF VELOCITY OF HORIZONTALLY POLARIZED SHEAR WAVE ON ROTATED Y-CUT BERLINITE

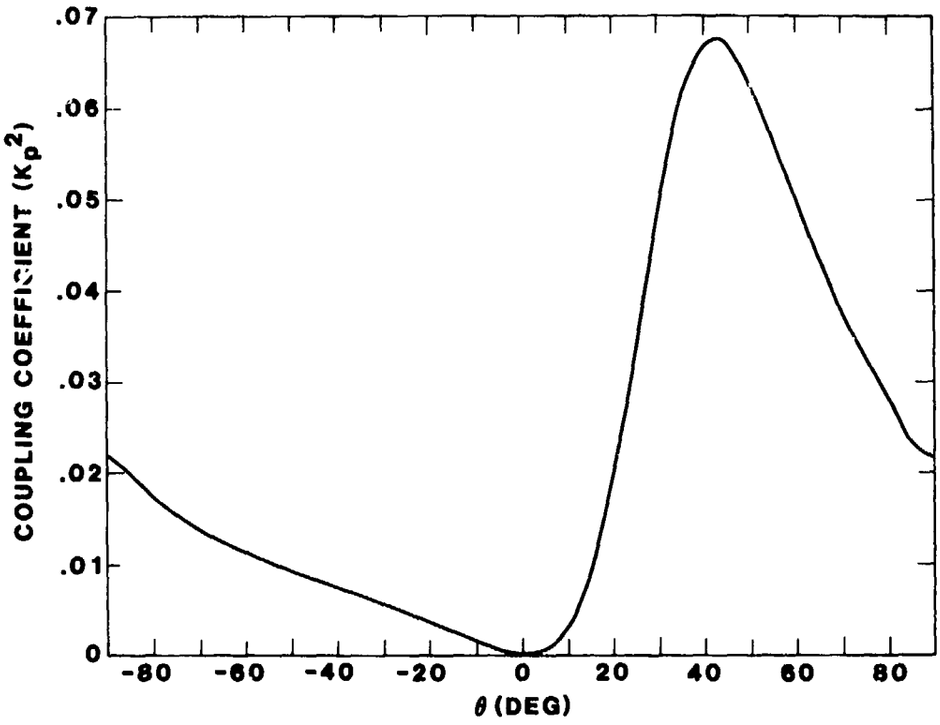

Figure 10. $\Delta v/v$ AND K_p^2 of SBAW IN ROTATED Y-CUT BERLINITE

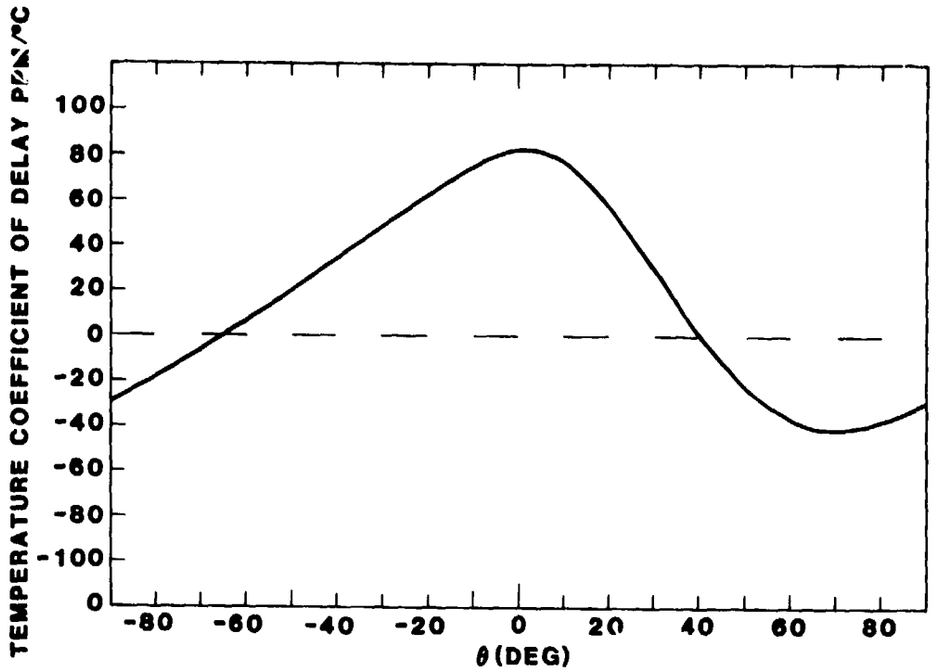

Figure 11. FIRST-ORDER TEMPERATURE COEFFICIENT OF DELAY OF SBAW IN ROTATED Y-CUT BERLINITE

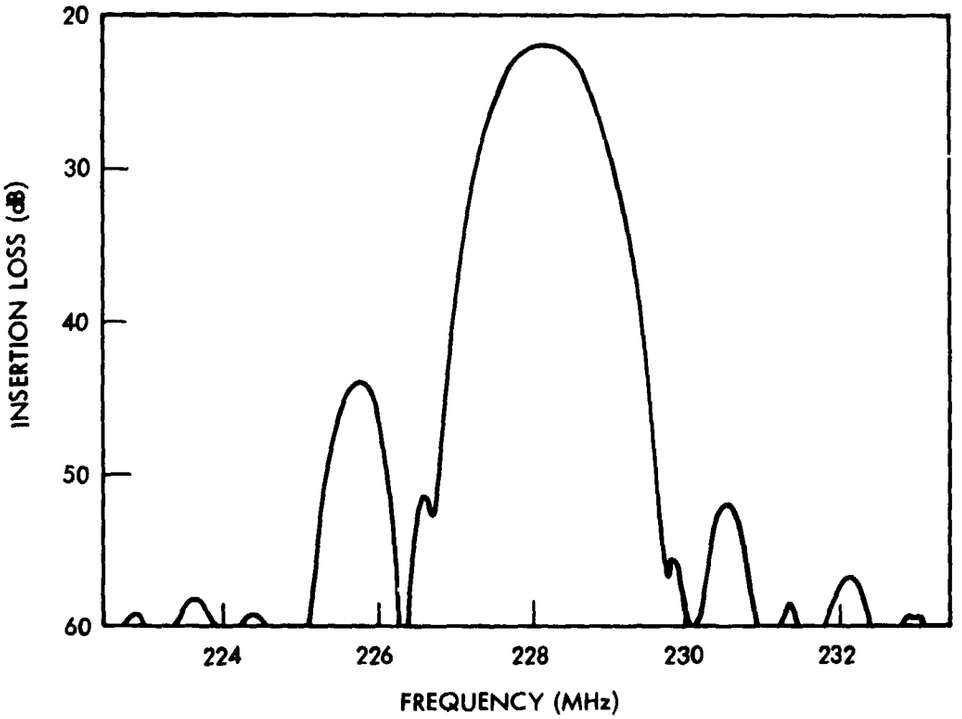

Figure 12. FREQUENCY RESPONSE OF SBAW DELAY LINE ON 40.5° ROTATED Y-CUT BERLINITE

The wave velocity as determined by the center frequency of the response was 4310 m/sec. This is compared to a theoretically predicted velocity of 4323 m/sec. Figure 13 summarizes the comparison between theory and experiment of the SBAW velocities for substrates with θ near 40.5°. The agreement is satisfactory. The discrepancy for the 40.5° and 41° devices can be attributed to metal loading effects, misalignment of transducers, and inaccurate crystal angles.

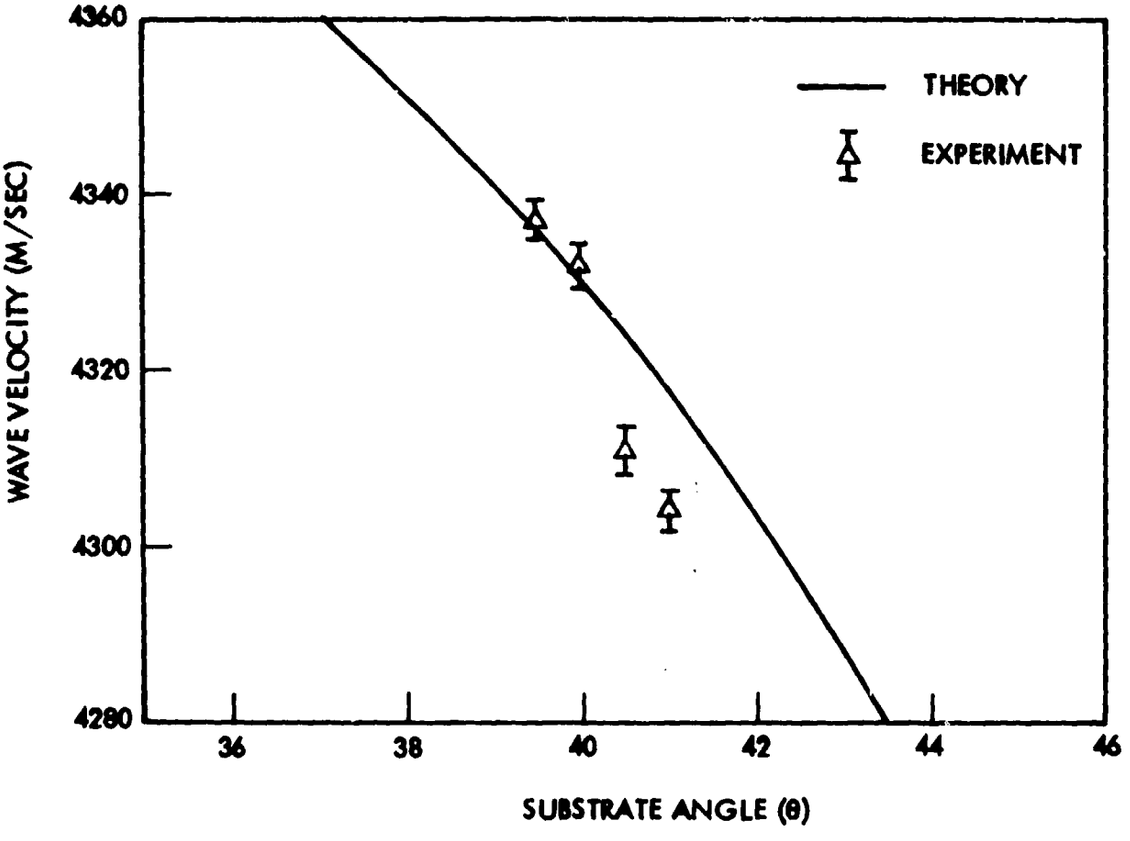

Figure 13. THEORETICAL AND EXPERIMENTAL DATA ON SBAW VELOCITY IN BERLINITE

The temperature stability of the SBAW device with θ near 40.5° was estimated theoretically based on published material constants and their temperature coefficients.[16] Since none of the third order coefficients were

available, all calculated results showed a parabolic dependence. As shown in Figure 14, the turnover temperature of the θ = 40.5° substrate was calculated to be at room temperature.

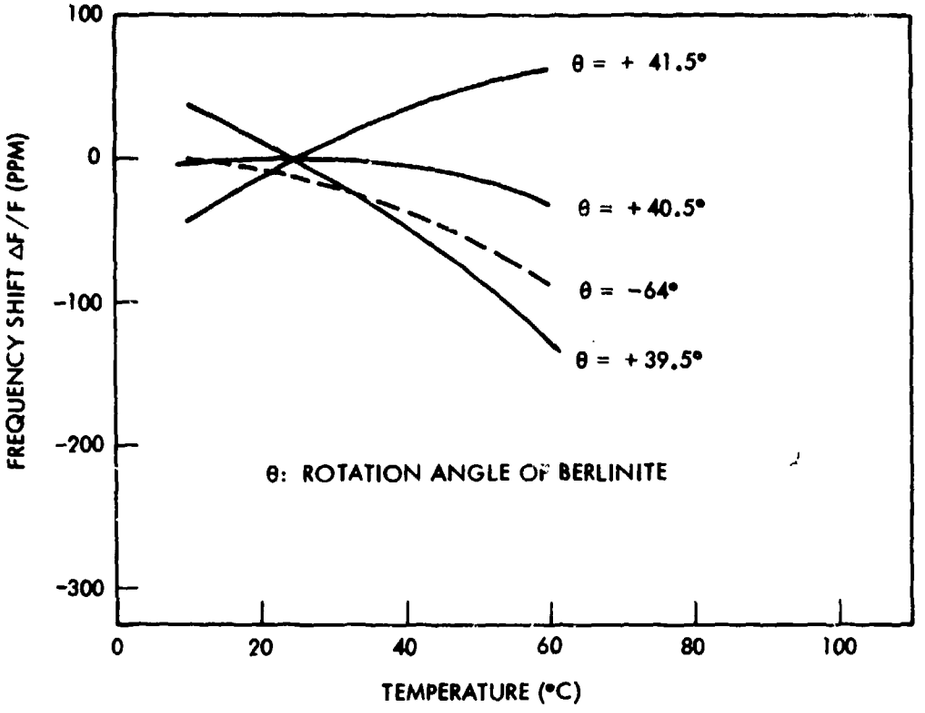

Figure 14. CALCULATED FREQUENCY - TEMPERATURE CURVES OF BERLINITE

The measured temperature behavior of the SBAW with θ near 40.5° is shown in Figure 15. These frequency-temperature curves turned out to be cubic functions. Zero first order coefficient occurred at temperatures between 50 and 60°C. It appeared that with smaller θ the turnover temperature shifted toward lower temperatures. This is in contrast with the calculated result which tends to indicate the opposite. It can be concluded from these measurements that some of the third and higher order terms in the temperature coefficient of material constants are significant and cannot be neglected. Furthermore, the symmetry of the third order coefficient of berlinite is different from that of quartz. In AT-cut quartz, the frequency-temperature curve of SBAW is parabolic.

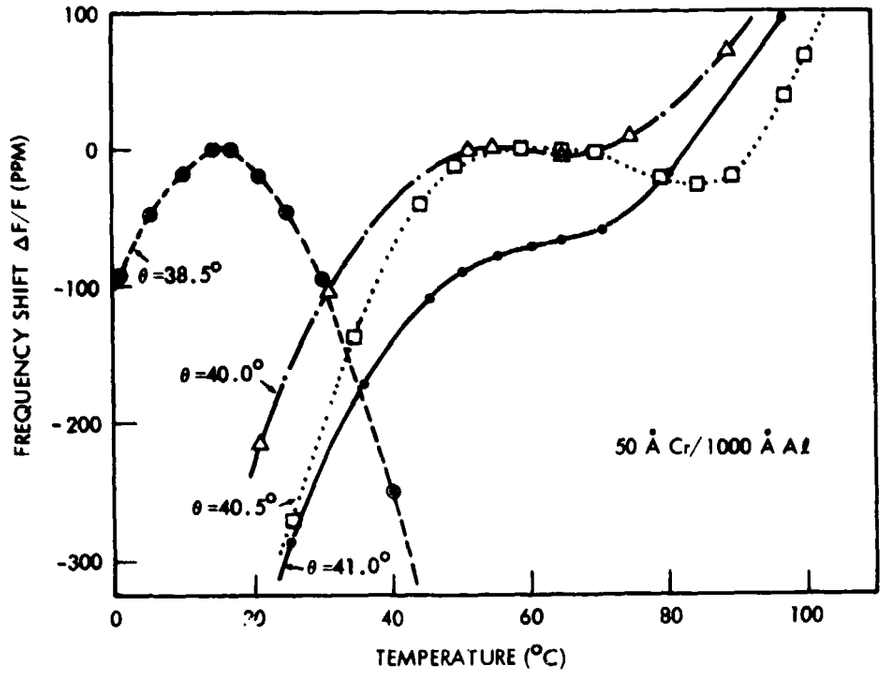

Figure 15. FREQUENCY - TEMPERATURE CURVES OF SBAW DEVICES ON BERLINITE WITH θ NEAR 40.5°

The temperature frequency curve was also dependent on the metal thickness. Figure 16 shows a measurement of the thickness dependence of the temperature characteristics of SBAW in 40.5° rotated Y-cut berlinite. The effect of metallization is to modify the flatness of the frequency-temperature curve. The device with thick metallization showed only 2.5 ppm shift in frequency over the temperature range of 15°C. This is comparable to the stability of SAW in ST-cut quartz for the same temperature range.

3.3.2 -64° Rotated Y-Cut Berlinite

The frequency response of the SBAW in -64° rotated Y-cut berlinite is shown in Figure 17. The wave velocity was measured to be 2893.6 m/sec, while calculations predicted a velocity of 2895.1 m/sec.

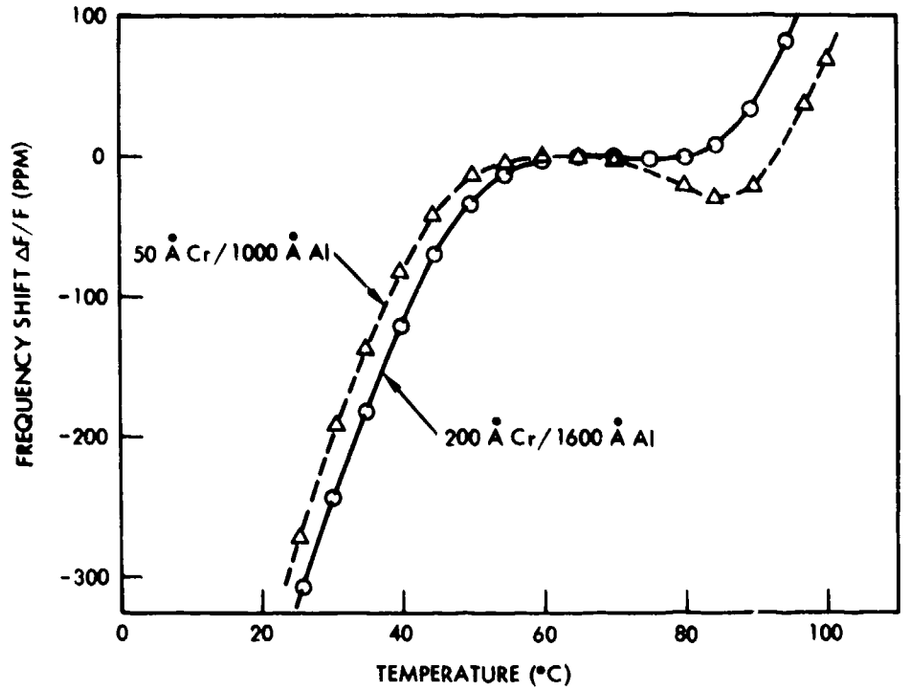

Figure 16. FREQUENCY TEMPERATURE CURVES OF SBAW DEVICES ON 40.5° ROTATED Y-CUT BERLINITE WITH TWO DIFFERENT METAL THICKNESSES

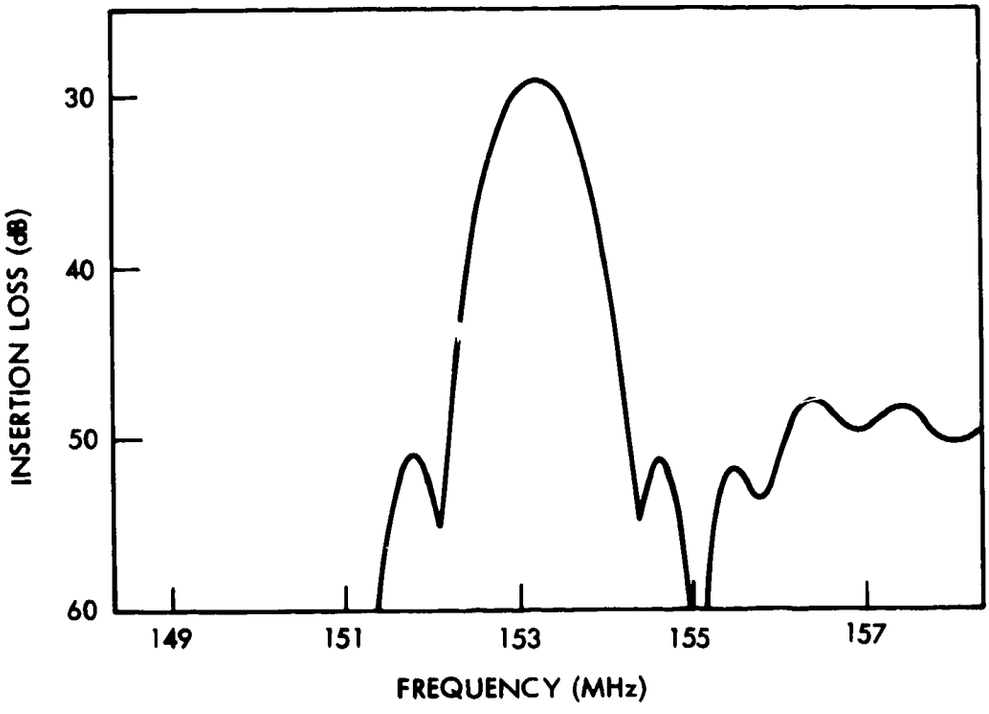

Figure 17. FREQUENCY RESPONSE OF SBAW DELAY LINE ON -64° ROTATED Y-CUT BERLINITE

The frequency-temperature curve of the SBAW device on -64° again showed a marked difference from that of SBAW on quartz, as shown in Figure 18. For SBAW on -50.5° rotated Y-cut quartz, the frequency temperature curve is a cubic function. In berlinite, the slow SBAW showed a parabolic dependence.

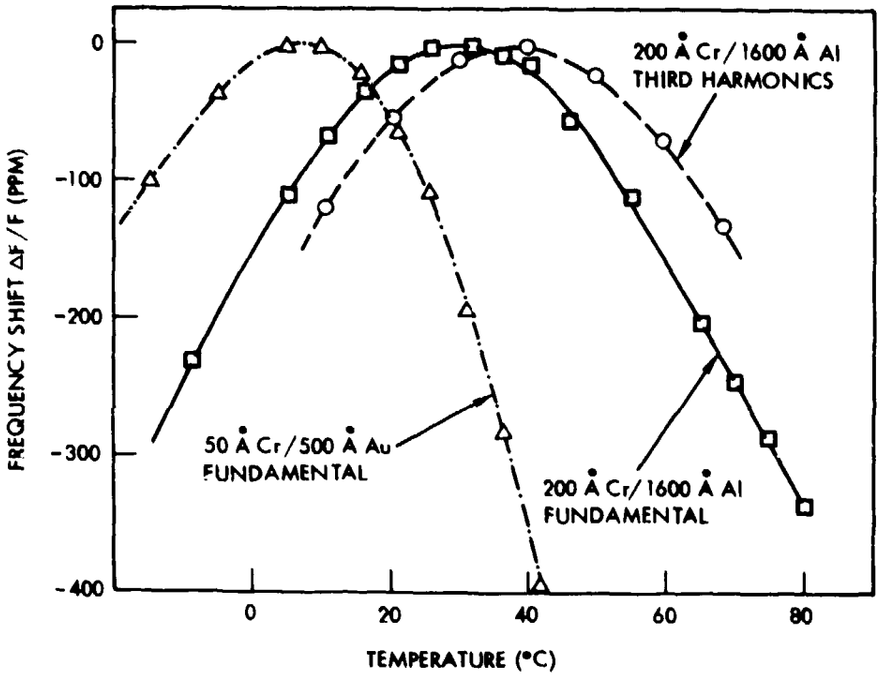

Figure 18. FREQUENCY-TEMPERATURE CURVES OF SBAW DEVICES ON -64° ROTATED Y-CUT BERLINITE

For quartz, the effect of Cr/Aℓ metallization is to lower the turnover temperature. In berlinite, it appeared to increase the turnover temperature. The 2nd order coefficient of delay for the Cr/Aℓ device was estimated to be approximately $190 \times 10^{-9}/°C^2$.

3.3.3 Coupling Coefficient

Our theoretical calculation indicates that berlinite possesses a higher piezoelectric coupling constant than that of quartz. This makes

berlinite an ideal material for temperature stable wideband SBAW devices. Therefore, the coupling coefficients of the berlinite substrate were evaluated, and the results summarized in Table 3. The measurements were not entirely consistent, which was attributed to quality of berlinite substrates. The numbers reported in Table 3 represent the best experimental values. The SBAW measurements indicated a much lower than theoretically predicted coupling for the 40.5° cut, while the coupling is close to theory for the -64° cut. These results are very encouraging because one can expect that a higher piezoelectric coupling coefficient can be obtained with improved material quality.

An independent check was performed by fabricating surface wave devices on 40.5° substrates and measuring their impedance and static capacitances. This measurement of the k^2 is considered to be more reliable since the equivalent circuit theory of surface wave devices is well understood. The coupling strength was measured to be half of that predicted by theory.

Table 3. ELECTROMECHANICAL COUPLING COEFFICIENT OF BERLINITE SAMPLES

Crystal Angle	Wave Type	Theory	Experiment
+40.5°	SAW	0.29%	0.15%
+40.5°	SBAW	6.7%*	1.5%*
-64°	SBAW	1.2%	1.0%*

*To obtain k^2, divide the number by the square root of N, where N is the number of finger pairs in the transducer.[2]

3.4 SBAW in $LiTaO_3$ and $LiNbO_3$

The crystal cuts on which SBAW devices are fabricated are 35° rotated Y-cut $LiTaO_3$ and 37° rotated Y-cut $LiNbO_3$. On these substrates, interdigital transducers are deposited such that SBAW propagate along the X-axis.

Our analysis has found that the equivalent circuit for SBAW devices on $LiTaO_3$ and $LiNbO_3$ is identical to the "cross-field" model for SAW. The piezoelectric coupling constants are determined to be 4.7% for 35° rotated Y-cut $LiTaO_3$ and 16.7% for 37° rotated Y-cut $LiNbO_3$. These values agree well with the result calculated using the velocity change between the SH bulk wave and the leaky surface wave under the metallized surfaces.

The first order temperature coefficient of delay has been calculated using shear horizontal waves along the surface. They are 45 ppm/°C and 59 ppm/°C for rotated 35° Y-cut $LiTaO_3$ and 37° Y-cut $LiNbO_3$, respectively. Thus, it is clear that SBAW on 35° rotated Y-cut $LiTaO_3$ has a high piezoelectric coupling constant and good temperature stability for wideband device application.

4.0 SBAW DEVICES

SBAW devices have been configured into bandpass filters, delay lines, oscillators and resonators. The results show that SBAW bandpass filters and oscillators are in many respects better than their SAW counterparts. They have higher frequency of operation, better temperature stability and better spurious bulk wave rejection. Here we will review some of the narrowband and wideband SBAW filters, and high frequency delay lines for oscillator applications. The demonstrated SBAW capabilities are shown in Table 4. In addition, we describe a SBAW energy trapping scheme which utilizes a grating. This configuration has significantly reduced the insertion loss of SBAW devices.

Table 4. DEMONSTRATED SBAW CAPABILITIES

Center Frequency	10 MHz to 3.4 GHz
Fractional Bandwidth	0.3% to 2% (Quartz) 15% $LiTaO_3$
Insertion Loss	13 dB
Sidelobe Suppression	> 55 dB
Shape Factor 3 dB/40 dB	1.4
Temperature Coefficient of Delay	0 for 1st and 2nd Order Coefficient

4.1 Narrowband SBAW Filters

Narrowband SBAW filters offer high frequency of operation, better temperature stability and low spurious modes. These filters were fabricated on various rotated Y-cuts of quartz. The propagation direction of the SBAW is normal to the X-axis. Both Hamming and sin x/x weighting functions have been used to weight the transducers to obtain the desired frequency response. Here, we will show some typical results.

Figure 19 shows the frequency response of a SBAW delay line fabricated on 125.7° rotated Y-cut quartz. The delay line consisted of a thinned electrode transducer and a Hamming function weighted transducer. The center frequency of this delay line is about 410 MHz, which is about 1.6 times higher than SAWs. The untuned insertion loss was about 25 dB and the

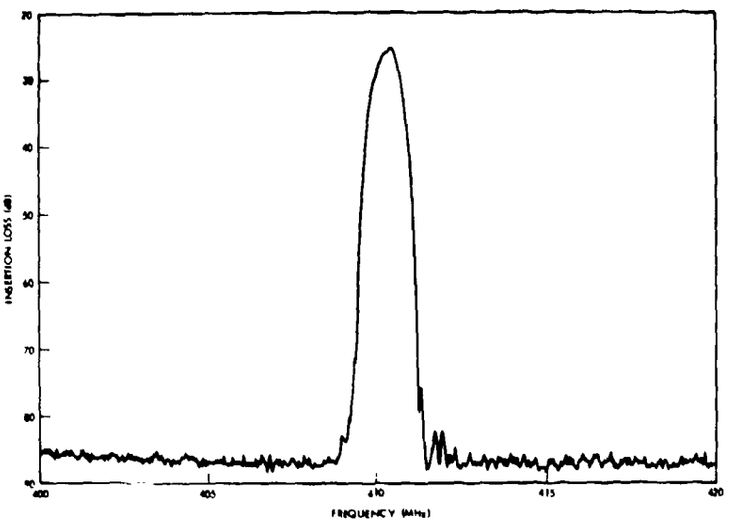

Figure 19. FREQUENCY RESPONSE OF SBAW DELAY LINE ON ROTATED Y-CUT QUARTZ USING THINNED ELECTRODE TRANSDUCER AND HAMMING FUNCTION WEIGHTED TRANSDUCER (λ = 0, μ = 125.7°, θ = 90°)

sidelobe rejection was about 60 dB. Figure 20 shows the frequency response on the same delay line over a wide frequency range. Note that there are no other spurious signals at higher frequencies. This is because the interdigital transducers excite and detect only the horizontally polarized shear wave or SBAW. This response is better than that of a SAW device using the same transducers.

4.2 Wideband SBAW Filters

Wideband SBAW delay lines were fabricated on $LiTaO_3$, which has a much higher piezoelectric coupling constant than that of quartz. These

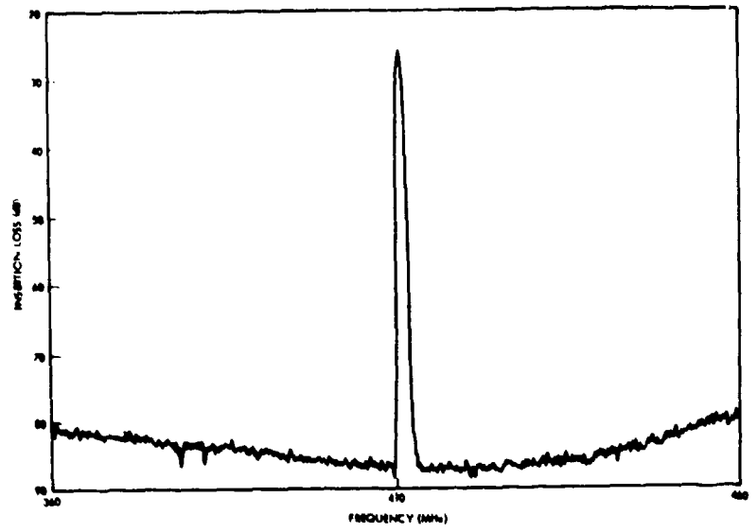

Figure 20. FREQUENCY RESPONSE OF SBAW DELAY LINE OVER A WIDE FREQUENCY RANGE (λ = 0, μ = 125.7°, θ = 90°)

wideband devices possess low temperature coefficient and low spurious modes.

Figure 21 shows the response of the SBAW delay line fabricated on 35° rotated Y-cut $LiTaO_3$. This wideband delay line filter consisted of two sin x/x apodized transducers and a multistrip coupler between. The fractional 3 dB bandwidth of this device was designed to be 15.4%. The number of strips in the multistrip coupler is 95 for optimal energy transfer. There were energy trapping strips outside the multistrip coupler, which had a stopband frequency at about 1.25 of the transducer center frequency for energy trapping. For this device, the untuned insertion loss is 23 dB, which agrees within 2 dB with the theoretical calculation using equivalent circuit model. However, the spurious bulk wave level at high frequencies is much lower than that of the SAW device with the same amount of back surface roughening.

4.3 Energy Trapping

Energy trapping techniques are extremely important in building high performance SBAW devices. Since the SBAW is a horizontally polarized shear wave which travels near the surface, it gradually spreads its energy

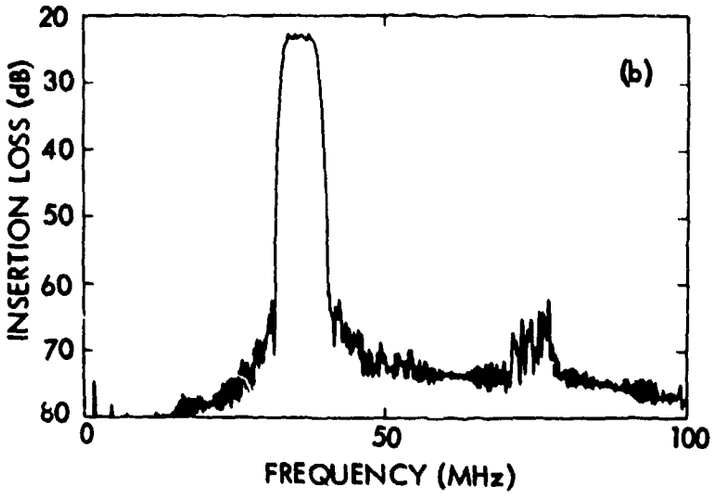

Figure 21. FREQUENCY RESPONSE OF THE BANDPASS FILTER FABRICATED ON 35° ROTATED Y-CUT $LiTaO_3$

into the bulk of the crystal. The spreading loss as a function of transducer separation can be calculated from Eq. (5). To reduce direct feedthrough, input and output transducers have to be separated relatively widely. This causes spreading loss. At TRW, we were the first to devise methods to completely eliminate this spreading loss. Suitable energy trapping schemes such as layered structure and grating have been employed. Here, we report the effect of a metallic grating on SBAW devices on quartz.[7]

A periodic metallic structure will support horizontal shear surface waves if the finger periodicity, d, is smaller than one-half of the SBAW wavelength, $d < \lambda_{SBAW}/2$.[7] Hence, a SBAW launched by the emitting transducer couples easily to the surface wave under the periodic metallization. The wave is "bound" to the surface, resulting in an enhanced signal received by the output transducer.

In experiments, the delay line consisted of one Hamming function apodized transducer and one finger withdrawal weighted transducer.[7] The center-to-center separation between transducers was 400 wavelengths. A metallic grating was placed between transducers. It consisted of 500 strips

and had a stopband at 1.25 times the center frequency of the device response. The grating was shorted to ground, which also suppressed the direct feedthrough signal.

Figure 22 shows the frequency response of the SBAW delay line on ST-cut quartz. The center frequency of operation was about 619 MHz. The device insertion loss was about 23 dB, and the sidelobe rejection was more than 55 dB. Without the metallic grating, the insertion loss increased by about 10 dB.

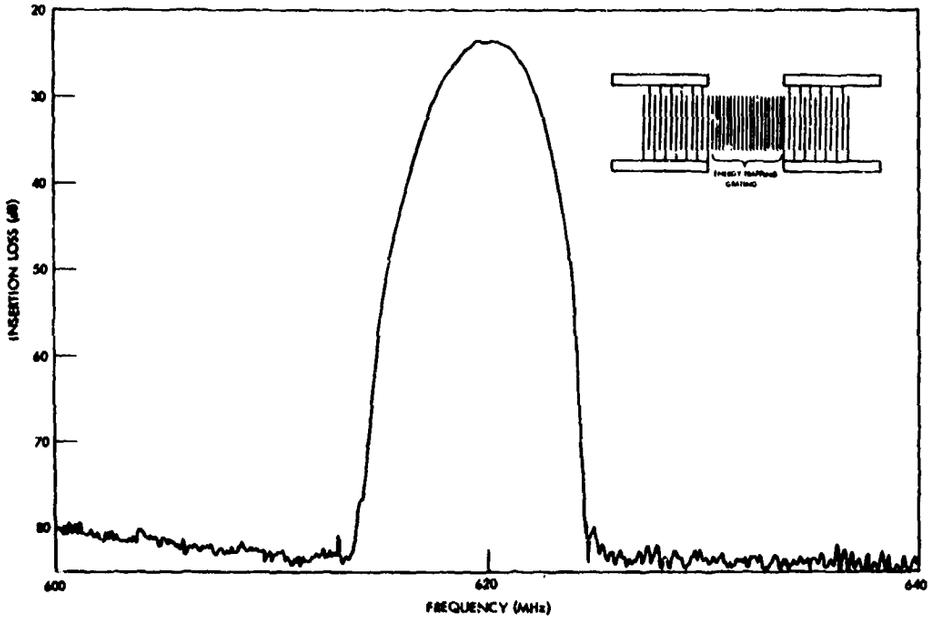

Figure 22. FREQUENCY RESPONSE OF UNTUNED SBAW FILTER WITH METALLIC GRATING

Figure 23 shows the response of the same device from 400 MHz to 1200 MHz. Note that no spurious bulk wave exists in this frequency range. This is because only the horizontally polarized shear wave is excited by the transducers. Thus, no elaborate bulk wave suppression is required to have high out-of-band rejection.

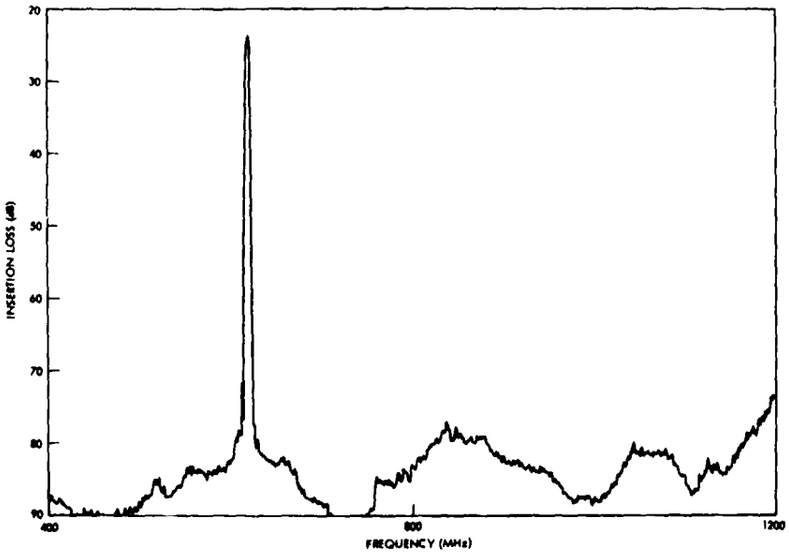

Figure 23. RESPONSE OF SBAW FILTER WITH METALLIC GRATING OVER A WIDE FREQUENCY RANGE

4.4 High Frequency SBAW Delay Line Oscillators[8]

Shallow bulk acoustic waves are very useful for high frequency oscillator applications due to their high wave velocity, low propagation loss, small temperature coefficient of delay and potentially better aging characteristics. To explore these superior characteristics, we have extensively investigated high frequency SBAW oscillators in this program. 2 GHz and 3.4 GHz SBAW delay lines were fabricated on rotated Y-cut quartz, and were used for direct frequency generation at 2 GHz and 3.4 GHz without using frequency multiplying circuits. These high frequency SBAW oscillators offer excellent phase noise and temperature stabilities. Their performance agreed very well with theoretical prediction. In addition, the 3.4 GHz oscillator represents the highest frequency source ever built with SAW and SBAW technologies.

4.4.1 2 GHz Delay Line

The 2 GHz delay line was designed with two identical uniform transducers operating at third harmonic. For devices at this frequency, the fingers must be embedded to reduce the insertion loss. Without embedded fingers, the insertion loss increased by approximately 10 dB.

The transducer configuration and the device response for a device fabricated on 35.5° rotated Y-cut quartz is shown in Figures 24a and 24b.

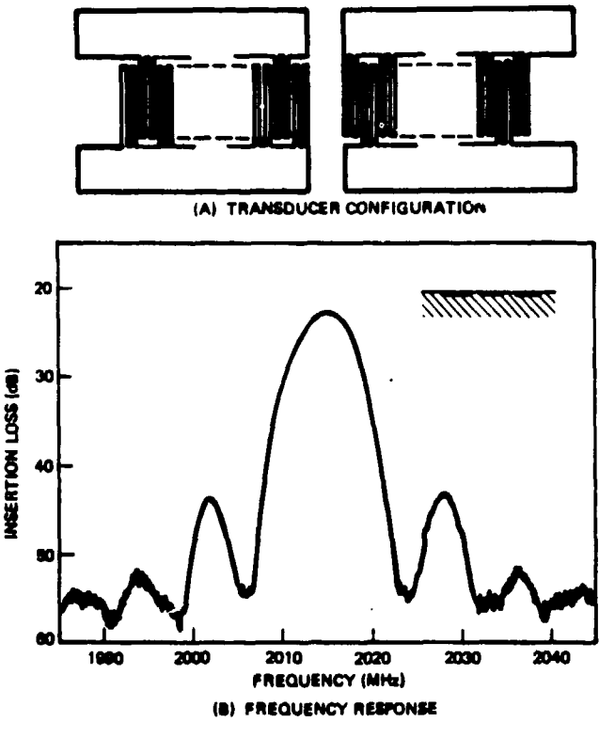

Figure 24. 2 GHz SBAW DELAY LINE ON 35.5° ROTATED Y-CUT QUARTZ (a) TRANSDUCER CONFIGURATION, (b) FREQUENCY RESPONSE

The device parameters are summarized in Table 5 and their unmatched insertion loss is 22.5 dB with 5.4 MHz bandwidth. The Q of the oscillator using this delay line would be approximately 900.

Table 5. 2 GHz SBAW DELAY LINE

Aperture	90 λ_o*
Finger Width	0.95 μm
Transducer Length	225 λ_o
Center-to-Center Separation Between Transducers	286 λ_o
Metallization	40 Å Ti/420 Å Aℓ
Groove Depth	400 Å

*Wavelength at third harmonic

4.4.2 3.4 GHz Delay Line

The 3.4 GHz delay line was designed to have fewer fingers and narrower apertures to offset losses due to finger edge diffraction and electrical mismatch. It utilizes a split finger design shown schematically in Figure 25. The design parameters are summarized in Table 6.

The 5th harmonic frequency response of the device fabricated on CT (38° rotated cut quartz) is shown in Figure 25. It has an unmatched insertion loss of 24 dB. Upon matching, it reduces to 22 dB. There are responses at the fundamental and third harmonic, but they are at least 10 dB down from the 5th harmonic response. The device has a center frequency of 3436 MHz, 3 dB bandwidth of 12.9 MHz, and a mode spacing of 14.5 MHz (Q = 750). Single mode oscillation is thus easily achieved.[8]

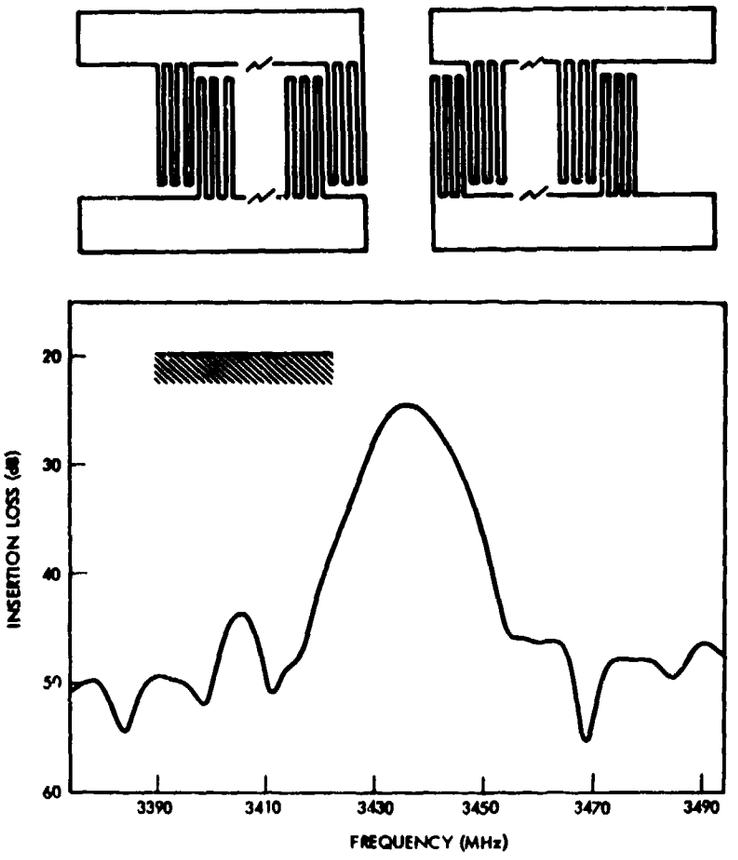

Figure 25. 3.4 GHz SBAW DELAY LINE ON CT QUARTZ.
(a) TRANSDUCER CONFIGURATION,
(b) FREQUENCY RESPONSE

Table 6. 3.4 GHz SBAW DELAY LINE

Aperture	75 λ_o*
Finger Width	0.61 μm
Transducer Length	168 λ_o
Center-to-Center Separation Between Transducers	240 λ_o
Metallization	300 Å Aℓ
Groove Depth	300 Å

*Wavelength at fifth harmonic

4.4.3 Oscillator Stability

The 2 GHz and 3.4 GHz SBAW delay lines were used to construct delay line oscillators. The oscillator circuit consisted of discrete components. This allows maximum flexibility in interchanging oscillator components and thus allows many delay lines to be incorporated and evaluated.

The stability of the SBAW oscillator has been investigated in regard to its phase noise and temperature coefficient of delay.

4.4.3.1 Phase Noise

For a delay line oscillator, the phase noise is described by the expression,[17]

$$\left[\frac{P_{sb}}{P_c}\right]_{\frac{dBc}{Hz}} = 10 \log \left[\frac{\alpha}{\omega^3 \tau^2} + \left(\frac{GFkT}{P_c}\right)\left(\frac{1}{\omega^2 \tau^2} + 1\right)\right], \qquad (7)$$

where

α = flicker noise parameter (sec^{-1})

τ = group delay

G = amplifier gain

F = noise figure

P_c = loop power

kT = thermal energy

This expression gives the FM signal-sideband noise power relative to the carrier in a 1 Hz bandwidth as a function of the Fourier or modulation frequency ω.

Application of this noise theory to the 2 and 3.4 GHz SBAW oscillator yields the theoretical results plotted in Figures 26 and 27. The parameters used in the calculation are summarized in Table 7.

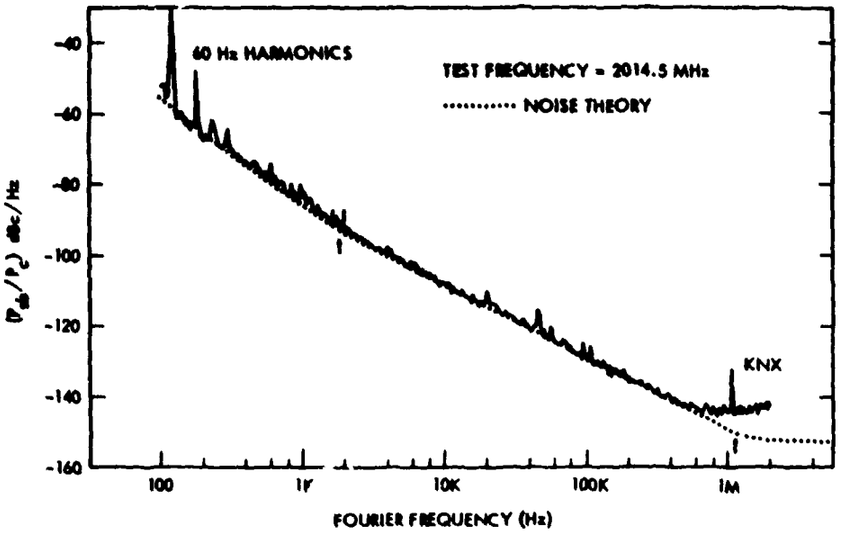

Figure 26. SINGLE SIDEBAND PHASE NOISE OF THE 2 GHz SBAW OSCILLATOR

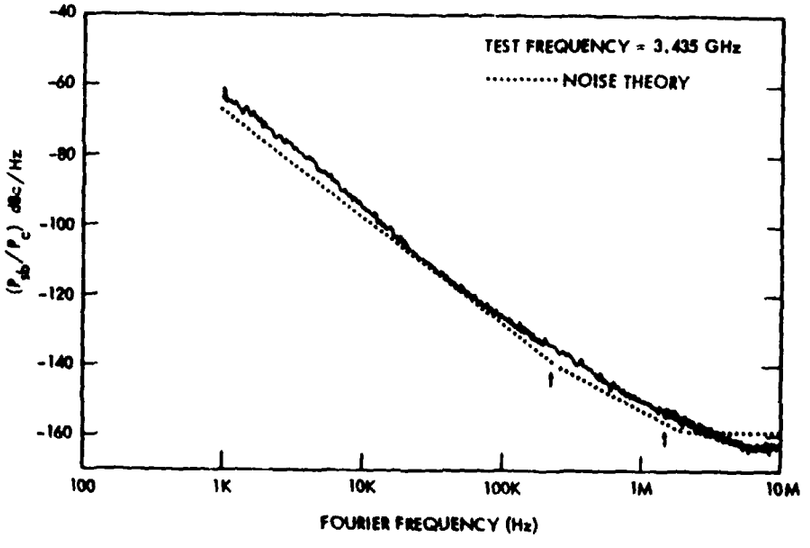

Figure 27. SINGLE SIDEBAND PHASE NOISE OF THE 3.4 GHz SBAW OSCILLATOR

Table 7. OSCILLATOR PARAMETERS

Oscillator Parameters		2 GHz Oscillator	3.4 GHz Oscillator
Amplifier Gain	G (dB)	25	24
Noise Figure	F (dB)	6	4
Loop Power	Pc (dB)	10	13
Group Delay	τ (μsec)	0.142	0.07
Flicker Noise Parameter	α (sec^{-1})	$6x10^{-12}$	$1.8x10^{-10}$

The experimental data are also plotted in Figures 26 and 27. These data are obtained at TRW Metrology using the single oscillator technique. The flicker noise parameter for the SBAW is comparable to that for SAW delay line oscillators.[18]

4.4.3.2 Temperature Coefficient of Delay

The temperature stability of the SBAW delay line oscillator is controlled by the temperature behavior of the SBAW delay line. For SBAW in rotated Y-cut quartz with θ near 36°, the temperature behavior is parabolic with zero first order coefficient of delay occurring at some turnover temperature T_o with a second order coefficient of delay of approximately $52x10^{-9}$/°C. The temperature behavior of three specific substrates is shown in Figure 28. The experimental data is taken with 2 GHz SBAW devices. Experimentally, the curves are all shifted toward lower temperatures from the theoretical values. The reason for this is that the substrate surface is covered by metal. Similar to the center frequency, the temperature characteristic of the SBAW delay line is affected by both the metal thickness and the percent of metal coverage. The effect of metallization is less severe

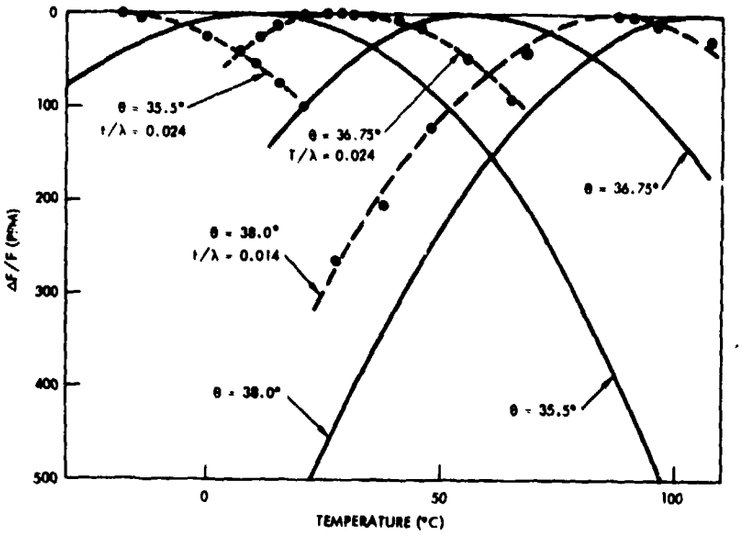

Figure 28. THEORETICAL AND EXPERIMENTAL TEMPERATURE BEHAVIOR OF SBAW DELAY LINE ON ROTATED Y-CUT QUARTZ

when the metal thickness-to-wavelength ratio is less than 0.02, causing less than 15°C lowering of the turnover temperature T_o.

5.0 CONCLUSIONS

This final report summarizes the most important results of the Investigation of Shallow Bulk Acoustic Waves (SBAW) program under ARO Contract DAAG26-78-C-0043. This program was conceived on the principle that SBAW technology could lead to devices that are superior to those presently available for frequency filtering and control. The primary objective was to establish whether this technology could provide devices that were as stable as the low frequency bulk wave resonators and yet operate at frequencies higher than the surface acoustic wave devices.

This program has clearly met all of these objectives. Our investigations have shown that SBAW devices can be built with excellent temperature stability, low spurious modes and at frequencies higher than those of SAW devices and bulk wave resonators.

We have extensively investigated shallow bulk acoustic waves in terms of material aspects, transducer equivalent circuits and device development. A complete understanding of SBAW properties, excitation, propagation, and detection, was necessary to establish SBAW technology and to allow the design of SBAW devices with specific characteristics.

Several acoustic wave materials were examined in this program. To date, the most promising substrate materials for SBAW devices are quartz, berlinite, $LiTaO_3$, and $LiNbO_3$. Quartz and berlinite possess zero first order temperature coefficients of delay and are therefore important materials for narrowband filters and oscillators. On the other hand, $LiTaO_3$ and $LiNbO_3$ possess high piezoelectric coupling constant for SBAW, making them excellent substrates for wideband devices.

In this program an equivalent circuit for SBAW transducers has also been developed. This eqivalent circuit provides the same simplicity in device design as that of the "cross-field" and "in-line" models for the surface acoustic wave devices. Experiments have confirmed the validity of this SBAW transducer model. This equivalent circuit has been routinely used to design SBAW devices.

Device development has clearly demonstrated that narrowband and wideband SBAW filters can be designed and fabricated with superior characteristics. The results show that SBAW devices are in many respects better than SAW devices, having higher frequency of operation, better temperature stability, and lower spurious modes. In addition, we have demonstrated that a metallic grating can significantly reduce the device insertion loss. SBAW devices with energy trapping can be used to produce superior bandpass filters with low insertion loss, high ultimate out-of-band rejection, and improved temperature stability.

Finally, shallow bulk acoustic waves are very useful for high frequency oscillator applications due to their high wave velocity, low propagation loss, excellent temperature stability and potentially better aging characteristics. We have extensively investigated high frequency SBAW oscillators in this program, and have constructed 2.0 GHz and 3.4 GHz SBAW oscillators with excellent phase noise and temperature stabilities. The 3.4 GHz oscillator also represents the highest frequency source ever built with SAW or SBAW technology. Our investigation also indicates that the frequency of operation can be easily extended to above 5 GHz.

BIBLIOGRAPHY

1. K.H. Yen, K.L. Wang and R.S. Kagiwada, "Efficient Bulk Wave Excitation on ST-Quartz", Electronics Letters, Vol. 13, pp 37-38 (1977).

2. K.Y. Yen, K.L. Wang and R.S. Kagiwada, "Interdigital Transducers - A Means of Efficient Bulk Wave Excitation", 31st Annual Frequency Control Symposium Proceedings (1977).

3. T.I. Browning and M.F. Lewis, "New Family of Bulk Acoustic Wave Devices Employing Interdigital Transducers", Electronics Letters, Vol. 13, pp 128-130 (1977).

4. M.R. Daniel, P.R. Emtage, and L. deKlerk, "Acoustic Radiation by Interdigital Grids on $LiNbO_3$", Proc. IEEE Ultrasonics Symposium, Oct. 1972.

5. V.M. Ristic, "Bulk Mode Generation in Surface Wave Devices", Proc. IEEE Ultrasonics Symposium, Oct. 1972.

6. R.S. Wagers, "Plate Mode Resonances in Surface Wave Delay Lines", Proc. IEEE Ultrasonics Symposium, Nov. 1973.

7. K.H. Yen, K.F. Lau, and R.S. Kagiwada, "Recent Advancement in Shallow Bulk Acoustic Wave Devices," 1979 Ultrasonics Symposium Proceedings.

8. K.F. Lau, K.H. Yen, R.S. Kagiwada, and A.M. Kong, "High Frequency Temperature Stable SBAW Oscillators," 1980 IEEE Ultrasonics Symposium Proceedings.

9. J. Wilcox, K.H. Yen and K.F. Lau, "Excitation of Shallow Bulk Acoustic Waves by Interdigital Transducers in Rotated Y-Cut Quartz", unpublished.

10. K. Yamanouchi and K. Shibayama, "Propagation and Amplification of Rayleigh Waves and Piezoelectric Leaky Waves in $LiNbO_3$", J. Appl. Phys., Vol. 43, No. 3, 1972, pp 856-862.

11. K. Nakamura, M. Kazumi and H. Shimizu, "SH-Type and Rayleigh Type Surface Waves on Rotated Y-Cut $LiTaO_3$", 1977 Ultrasonics Symposium Proceedings.

12. A. Ballato and T. Lukaszek, "Shallow Bulk Acoustic Wave Devices", 1979 MTT Symposium Digest, pp 162-164.

13. A. Ballato, T. Lukaszek, K.H. Yen, and R.S. Kagiwada, "SAW and SBAW on Doubly Rotated Cut Quartz", Proc. IEEE Ultrasonics Symp., Sept. 1979.

14. J. Wilcox and K.H. Yen, "Shear Horizontal Surface Wave on Rotated Y-Cut Quartz", to be published in IEEE Trans. on Sonics and Ultrasonics.

15. R. Beckman, A.D. Ballato and T.J. Lukaszek, "Higher-Order Temperature Coefficients of the Elastic Stiffnesses and Compliances of Alpha-Quartz", Proc. IRE, Vol. 50, No. 8, August 1962.

16. Z.P. Chang and G.R. Barsh, IEEE Trans. on Sonics and Ultrasonics, SU-23, p. 127 (1976).

17. T.E. Parker, "Current Developments in SAW Oscillator Stability," Proc. 31st Annual Freq. Control Symp., 1977.

18. T.E. Parker, "1/f Phase Noise in Quartz SAW Devices," Proc. IEEE Ultrasonics Symp., 1979.

PUBLICATIONS UNDER ARO PROGRAM

1. K.F. Lau, K.H. Yen, J.I. Wilcox and R.S. Kagiwada, "Analysis of Shallow Bulk Acoustic Wave Excitation by Interdigital Transducers", Proc. 33rd Annual Freq. Control Symp., 1979, Atlantic City, NJ.

2. K.H. Yen, K.F. Lau and R.S. Kagiwada, "Narrowband and Wideband Shallow Bulk Acoustic Wave Filters", Proc. IEEE International Symp. on Circuits and Systems, Japan, 1979.

3. K.H. Yen, K.F. Lau and R.S. Kagiwada, "Recent Advancement in Shallow Bulk Acoustic Wave Devices", 1979 Ultrasonics Symp. Proc.

4. A. Ballato, T. Lukaszek, K.H. Yen and R.S. Kagiwada, "SAW and SBAW on Doubly Rotated Cut Quartz", Proc. 1979 Ultrasonics Symp.

5. K.F. Lau, K.H. Yen, R.S. Kagiwada and A.M. Kong, "A Temperature Stable 2 GHz SBAW Delay Line Oscillator", Proc. 34th Annual Freq. Control Symp., US Army Electronics Technology and Device Lab, Fort Monmouth, NJ, May 1980.

6. K.F. Lau, K.H. Yen, R.S. Kagiwada and A.M. Kong, "High Frequency Temperature Stable SBAW Oscillators", 1980 IEEE Ultrasonics Symp. Proc.

7. K.F. Lau, K.H. Yen, R.S. Kagiwada and B.H.T. Chai, "Shallow Bulk Acoustic Wave in Berlinite", Proc. 35th Annual Freq. Control Symp., US Army ET&D Lab, Fort Monmouth, NJ, 1981.

8. K.F. Lau, R.F. Stokes, K.H. Yen, and B.H.T. Chai, "Investigation of Temperature Stable SBAW in Berlinite", 1981 Ultrasonics Symp., Chicago.

9. J. Wilcox and K.H. Yen, "Shear Horizontal Surface Wave on Rotated Y-Cut Quartz", to be published in IEEE Trans. on Sonics and Ultrasonics.